Interfacial Properties of Model Membranes and Plasma Lipoproteins Containing Ether Lipids†

John B. Massey, Hoyan S. She, and Henry J. Pownall*
Department of Internal Medicine, Baylor College of Medicine, and The Methodist Hospital, Houston, Texas 77030
Received May 22, 1985

ABSTRACT: The interfacial properties of synthetic ester and ether phosphatidylcholines (PCs) were investigated by using the polarity-sensitive fluorescent probes 6-propionyl-2-(dimethylamino)naphthalene (Prodan) and pyrene. The physical state of the phospholipid matrix was determined by fluorescence polarization of 1,6-diphenyl-1,3,5-hexatriene (DPH). Single-bilayer phospholipid vesicles formed by sonication and model high-density lipoproteins were studied. On the basis of a number of spectroscopic and thermodynamic criteria, the interfacial regions of PCs and their ether analogues are similar. The fluorescence properties of Prodan in model lipoproteins or single-bilayer vesicles were independent of the phospholipid fatty acyl chain length and polar head group, as well as the substitution of ether linkage for ester bonds in the phospholipid. The spectral shifts correlated mainly with the physical state of the phospholipid. The emission spectrum of Prodan appeared at shorter wavelengths upon transfer from water to liquid-crystalline phospholipid and blue shifted further when the lipid was cooled to its gel phase. The effect of cholesterol in model high-density lipoproteins on the emission spectrum of Prodan was dose dependent and, at 18 mol % cholesterol, the spectrum was similar to that observed in a pure gel-phase lipid and was independent of temperature. The quantum yield of Prodan fluorescence in an ether–PC matrix was similar to that observed in water, whereas in an ester–PC matrix it was enhanced by a factor of about 5. Phospholipid–water partition coefficients of Prodan were independent of the physical state of 1,2-dimyristoyl-*sn*-glycero-3-phosphocholine or 1,2-tetradecyl-*sn*-glycero-3-phosphocholine. In ether and ester PCs, changes in the enhancement ratio of the vibronic bands of pyrene corresponded with the lipid-phase transition. The quantum yield of pyrene was greatly enhanced when an ester–PC matrix was replaced by an ether–PC matrix. Spectral differences of the probes in gel vs. liquid-crystalline phases are consistent with differences in exclusion or entry of water into the interfacial region due to lateral expansion of the head groups. The observed effects with cholesterol are consistent with dehydration of the probe environment. The decreased quantum yield of Prodan, pyrene, and DPH in ether phospholipids suggests that greater water penetration creates a hydrophobic–hydrophilic balance in the interface for ether phospholipids that is comparable to that of ester phospholipids. Therefore, proteins and other amphiphiles that associate with the phospholipid surfaces via the interfacial hydrophobic effect should not distinguish between diacyl- and dialkylglycerophosphocholines.

Lipolytic enzymes, lipid transfer proteins, apolipoproteins, and certain membrane-bound proteins associate with the phospholipid–water interface. The properties of this region are key determinants of the initial association, the stability of the complex, and probably the function of these proteins in the phospholipid matrix. The polarity and dielectric constant of the interfacial region of phospholipids are distinct from those of the bilayer interior (Griffith et al., 1974; Schmidt et al., 1977; Ashcroft et al., 1981; Bellemare & Fragata, 1980), and the polarity or hydration of the lipid–water interface has been suggested to regulate the thermodynamics of protein–phospholipid association (Pownall et al., 1981b, 1982b; Misiorowski & Wells, 1974). In addition, these surface factors might modulate the activity or lipophilicity of proteins and other amphiphiles that locate at the phospholipid–water interface in membranes and lipoproteins.

We have investigated the nature of the surface region of model membranes and lipoproteins using the polarity-sensitive fluorescent probes 6-propionyl-2-(dimethylamino)naphthalene (Prodan)[1] (Weber & Farris, 1979) and pyrene (Georghiou & Mukhopadhyay, 1981). The physical state of the phospholipid matrix was determined by fluorescence polarization of DPH (Mantulin et al., 1981). Model high-density lipoproteins were studied because they contain only the surface components (apolipoprotein, phospholipid, and cholesterol) (Shen et al., 1977) and are a well-characterized system (Tall et al., 1975; Jonas & Mason, 1981; Massey et al., 1981). Single-bilayer vesicles produced by sonication were used as a simple model bilayer membrane (Barenholz et al., 1977).

Experimental Procedures

Materials. DMPC, DMPG, DMPA, DLPC, DPPC, and cholesterol were purchased from Calbiochem (La Jolla, CA).

† This research was supported by grants from the National Institutes of Health (HL-26250, HL-30914, HL-27341, and HL-30913) and by a grant from the Robert A. Welch Foundation (Q-906 to H.J.P.).

* Address correspondence to this author at the Department of Internal Medicine, Baylor College of Medicine.

[1] Abbreviations: DMPC, 1,2-dimyristoyl-*sn*-glycero-3-phosphocholine; DMPC ether, 1,2-ditetradecyl-*sn*-glycero-3-phosphocholine; DMPA, 1,2-dimyristoyl-*sn*-glycero-3-phosphatidic acid; DMPG, 1,2-dimyristoyl-*sn*-glycero-3-phosphoglycerol; SM, egg yolk sphingomyelin; DLPC, 1,2-dilauroyl-*sn*-glycero-3-phosphocholine; DPPC, 1,2-dipalmitoyl-*sn*-glycero-3-phosphocholine; HDL, high-density lipoprotein(s); apoA-I, apolipoprotein A-I (the major protein in human HDL); SBV, single-bilayer vesicles; Prodan, 6-propionyl-2-(dimethylamino)-naphthalene; DPH, 1,6-diphenyl-1,3,5-hexatriene; K_p, lipid–water partition coefficient; TNS, 6-(*p*-toluidino)naphthalene-2-sulfonic acid; apoA-II, apolipoprotein A-II (the second most abundant protein in human HDL); HPLC, high-performance liquid chromatography; T_c, temperature of the gel → liquid-crystalline phase transition; Patman, 6-palmitoyl-2-[[[2-(trimethylammonio)ethyl]methyl]amino]naphthalene chloride; EDTA, ethylenediaminetetraacetic acid; Tris, tris(hydroxymethyl)aminomethane; RPM, relative polarity measurement.

0006-2960/85/0424-6973$01.50/0

Egg yolk sphingomyelin was from Avanti Polar Lipids (Birmingham, AL). Prodan was from Molecular Probes (Grand Junction, OR), and pyrene was from Aldrich Chemical Co. DMPC ether was synthesized by standard procedures (Eibl, 1981). ApoA-I was purified as previously described (Pownall et al., 1981a). Model-reassembled HDL composed of apoA-I and different phospholipids was formed spontaneously by incubation at the transition temperature of the lipid or by cholate dialysis (Pownall et al., 1981a, 1982a; Matz & Jonas, 1982). The model HDL had an average lipid to protein molar stoichiometry of 100/1. Single-bilayer vesicles were formed by sonication (Barenholz et al., 1977). Spectral or HPLC-grade solvents were from usual vendors. Protein concentrations were routinely determined by absorption spectroscopy and phospholipid concentration by the method of Bartlett (1959). A standard buffer composed of 0.1 M NaCl, 1 mM NaN_3, 1 mM EDTA, and 0.01 M Tris, pH 7.4, was used throughout.

Fluorescence Methods. Corrected fluorescence spectra and fluorescence polarization (Mantulin et al., 1981) were measured on an SLM Instruments 8000 spectrofluorometer (Urbana, IL). The relative quantum yields were determined by measuring the area enclosed by the fluorescence spectra. Samples were kept at constant temperature via a circulating water bath, and sample temperatures were measured directly in the cuvette with a Bailey BAT 8 digital thermometer.

The partition coefficient for the distribution of Prodan between phospholipid and water is given by

$$K_p = \frac{\text{mol of bound probe/mol of phospholipid}}{\text{mol of free probe/mol of } H_2O} \quad (1)$$

and was determined by titration of a constant amount of fluorescent probe with varying concentrations of a model lipoprotein. The data were analyzed by a plot (Sklar, 1980) of

$$1/I = (1/K_p)(1/I_{max})(\text{mol of } H_2O/\text{mol of PC}) + 1/I_{max} \quad (2)$$

where K_p is the partition coefficient, I is the fluorescence intensity at a given molar ratio of H_2O to lipid, and I_{max} is the maximal fluorescence intensity change.

The Prodan fluorescence spectra were measured and analyzed for the wavelength of maximal fluorescence intensity and spectral width. By use of the K_p values in Table I, conditions were selected so that >99% of the probe was associated with phospholipid. Spectral width at half-maximal intensity ($\Delta\nu_{1/2}$) was determined by

$$\Delta\nu_{1/2} = \frac{1}{(\text{wavelength})_2} - \frac{1}{(\text{wavelength})_1} \text{ cm}^{-1} \quad (3)$$

where the two wavelengths correspond to the points of intersection of the emission spectrum with a line corresponding to 50% of the maximum intensity. The wavelength maxima and $\Delta\nu_{1/2}$ of Prodan were determined in methanol, ethanol, dimethyl sulfoxide, chloroform, ethyl acetate, tetrahydrofuran, benzene, ethyl ether, hexane, and buffer. The results were similar to those previously published (Weber & Farris, 1979). A plot of wavelength maxima was linear with the polarity of the solvent. The relative polarity measurement (RPM) for the various solvents was used because it is a dimensionless parameter which easily allows comparisons between solvatochromic dyes (Reichardt, 1979). Values for $\Delta\nu_{1/2}$ for each of the solvents were approximately 3000 cm^{-1}.

The enhancement ratios of the vibronic bands of pyrene fluorescence, which are sensitive to the environment of the molecule (Georghiou & Mukhopadhyay, 1981), were calculated as the ratio of the intensity at 376 nm (I_{376}) to that observed at 387 nm (I_{387}).

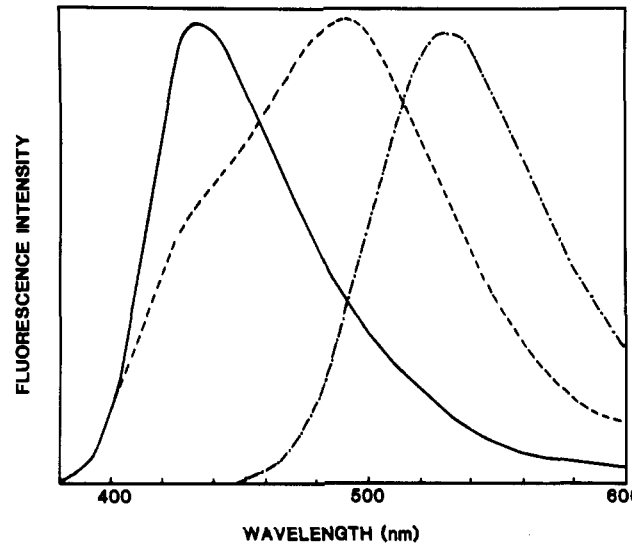

FIGURE 1: Fluorescence spectra of Prodan were determined in buffer (-·-) and in apoA-I/DMPC at 15 (—) and 37 °C (- - -). Prodan, in ethanol, was added to 1.5 mL of buffer or to 1.5 mL of a 1 mg/mL phospholipid solution of model HDL. The final concentration of Prodan was 5 μM.

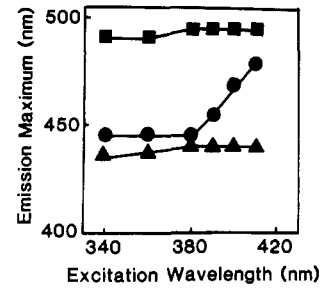

FIGURE 2: Fluorescence emission maxima of Prodan in a model lipoprotein, apoA-I/DMPC, were measured as a function of the excitation wavelength. The measurements were made at 15 (▲), 30 (●), and 45 °C (■).

RESULTS

Spectroscopy of Prodan in Model HDL. The fluorescence of Prodan bound to a model HDL containing DMPC and apoA-I was temperature dependent. The association of Prodan with a liquid-crystalline phospholipid matrix at 37 °C gave a fluorescence spectrum that was blue shifted compared to that in observed buffer (Figure 1). Decreasing the temperature to 15 °C, where the lipid is in the gel phase (Tall et al., 1977), further increased the blue shift of the spectrum. By contrast, the fluorescence spectrum of Prodan in buffer was independent of temperature between 15 and 37 °C.

For both gel- (T = 15 °C) and fluid-phase (T = 45 °C) phospholipid in model HDL, the emission maximum of Prodan was independent of the excitation wavelength (Figure 2). At 30 °C, where gel- and fluid-phase lipids coexist, there was a red shift in the emission maxima as a function of increasing excitation wavelength; however, $\Delta\nu_{1/2}$ was constant over the same wavelength range.

The partition coefficient, K_p, for Prodan distribution between phospholipid and water was measured. The lipid phases were composed of apoA-I and DMPC, apoA-I and DMPC ether, and single-bilayer vesicles of DMPC or DMPC ether (Table I). At a given temperature, the observed K_p with the model HDL varied 2-fold. At 15 and 37 °C, K_p differed by less than a factor of 2. As expected, the free energies of transfer of

Table I: Partition Coefficients and Quantum Yields for Prodan in Model Lipoproteins and Single-Bilayer Vesicles[a]

system	T_c (°C)	$K_p \times 10^{-5}$ at 15 °C	$K_p \times 10^{-5}$ at 37 °C	ΔG (kcal/mol) at 15 °C	ΔG (kcal/mol) at 37 °C	rel quantum yield at 15 °C	rel quantum yield at 37 °C
apoA-I/DMPC	27	4.3	3.3	−7.4	−7.8	4.3	5.9
apoA-I/DMPC ether	30	3.6	2.2	−7.3	−7.6	1.0	1.1
DMPC SBV	22	8.0	3.8	−7.8	−7.9	3.0	4.7
DMPC ether SBV	25	3.8	4.8	−7.4	−8.1	0.5	0.6

[a] T_c is the midpoint of the gel–liquid-crystalline phase transition as measured by fluorescence polarization. K_p is the lipid–water partition coefficient. ΔG is the free energy of transfer ($\Delta G = -RT \ln K_p$). The relative quantum yield is calculated as the integrated fluorescence intensity of the bound probe divided by the intensity of the same concentration of Prodan in buffer. Other details are found under Experimental Procedures.

Table II: Effect of Lipid Composition on the Fluorescence Properties of Prodan in Model Lipoproteins[a]

model lipoprotein	wavelength max (nm) at 15 °C	wavelength max (nm) at 40 °C	RPM at 15 °C	RPM at 40 °C	$\Delta\nu_{1/2}$ (cm^{-2}) at 15 °C	$\Delta\nu_{1/2}$ (cm^{-2}) at 40 °C
apoA-I/DMPC	435	493	−0.26	−0.68	3600	4500
apoA-I/DMPG	434	498	−0.24	−0.71	3800	5640
apoA-I/DMPA	439	484	−0.29	−0.61	4300	6150
apoA-I/DMPC ether	442	484	−0.30	0.61	5200	6250
apoA-I/SM	430	492	−0.22	−0.67	4800	5500
apoA-I/DMPC/6 mol % cholesterol	434	492	−0.25	−0.67	3500	5400
apoA-I/DMPC/12 mol % cholesterol	434	491	−0.24	−0.66	3550	5400
apoA-I/DMPC/18 mol % cholesterol	433	438	−0.23	−0.28	3150	5000
DMPC SBV	437	492	−0.27	−0.67	4500	3900
DMPC ether SBV	419	488	−0.14	−0.64	3640	5900
SM SBV	433	485	−0.24	−0.62	5650	4100
apoA-I/DLPC	442	494	−0.30	−0.68	5250	4200
apoA-I/DPPC	439	470	−0.28	−0.51	3950	5200

[a] RPM is the relative polarity measurement, and $\Delta\nu_{1/2}$ is the spectral width at half-maximal intensity as defined under Experimental Procedures.

Prodan from the model lipoproteins to water were approximately the same.

Comparison of Prodan in DMPC and Model HDL. The wavelength maxima and $\Delta\nu_{1/2}$ for Prodan and the fluorescence polarization of DPH (Figure 3) were each a sensitive indicator of the phase transition of DMPC. The abrupt change in the emission maximum of Prodan and the change in DPH polarization both coincided with the gel to liquid-crystalline transition. The emission maximum of Prodan fluorescence in the gel and fluid phases was not changed by the presence of apoA-I (Figure 3A). In the model HDL, the changes in DPH polarization and Prodan fluorescence maximum were both about 5 °C higher than the corresponding changes in SBV. The width of the spectra ($\Delta\nu_{1/2}$) varied with temperature and passed through a maximum in the region of the phase transition. The $\Delta\nu_{1/2}$ values of Prodan fluorescence in phospholipid matrices are several hundred wavenumbers greater than those observed in neat organic solvents (~3000 cm^{-1}).

Effects of Lipid Composition of Model HDL on Prodan Fluorescence. The temperature dependence of the Prodan fluorescence maximum in model HDL composed of apoA-I and DMPC ether was similar to that for those containing DMPC. The limiting value of the maximum for gel-phase lipid was lower for DMPC ether SBV. The addition of cholesterol to the model produced profound changes in the temperature dependence of the emission maxima of Prodan. At 18 mol % cholesterol (Figure 3G), the emission maxima of Prodan remained constant with increasing temperature. The temperature at which the maximum value of $\Delta\nu_{1/2}$ is observed increased with increasing cholesterol content.

The fluorescence properties of Prodan in model HDL were measured as a function of lipid composition. The variables were fatty acyl chain length, head group (DMPC, DMPA, DMPG), cholesterol content, glycero esters and glycero ethers (Table II). Single-bilayer vesicles of DMPC, DMPC ether, and sphingomyelin were also used. The wavelength maxima differed only slightly at 15 and 40 °C for all the complexes

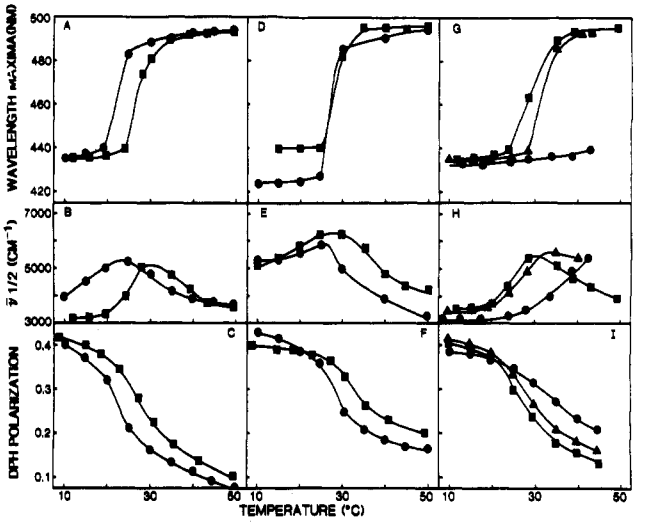

FIGURE 3: Fluorescence parameters of Prodan and DPH were determined in model HDL. The fluorescence spectra of Prodan were analyzed by the wavelength at maximal fluorescence intensity (panels A, D, and G) and by the spectral half-width ($\Delta\nu_{1/2}$)(panels B, E, and H). To verify the physical state of the lipid, the polarization of DPH fluorescence was also measured (panels C, F, and I). Model HDL composed of apoA-I and DMPC (■) and of DMPC SBV (●) (panels A–C); model HDL composed of apoA-I and DMPC ether (■) and of DMPC ether SBV (●) (panels D–F); model apoA-I, DMPC, and cholesterol containing 6 (■), 12 (▲), and 18 (●) mol % cholesterol (panels G–I).

studied. Spectral maxima for Prodan in ethyl acetate and ethanol were comparable to those in gel- (T = 15 °C) and fluid-phase lipid (T = 40 °C), respectively. The relatively large values of $\Delta\nu_{1/2}$ were consistent with spectral heterogeneity related to the physical state of the lipid.

Effects of Microenvironment on Pyrene Fluorescence. The ratios of the fluorescence intensity of the vibronic bands of pyrene are sensitive to the environment of the molecule. In model HDL or vesicles composed of DMPC or DMPC ether,

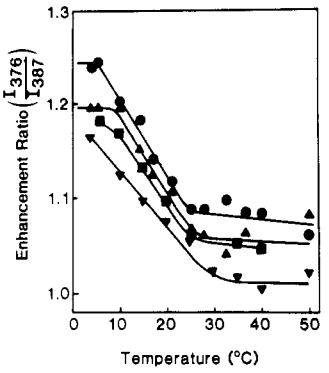

FIGURE 4: Spectral properties of pyrene in model HDL composed of apoA-I and DMPC (●) and of apoA-I/DMPC ether (▲) and in SBV composed of DMPC (■) and of DMPC ether (▼) as a function of temperature. The measured ratio is that of the fluorescence intensity at 376 nm (I_{376}) to that observed at 387 nm (I_{387}).

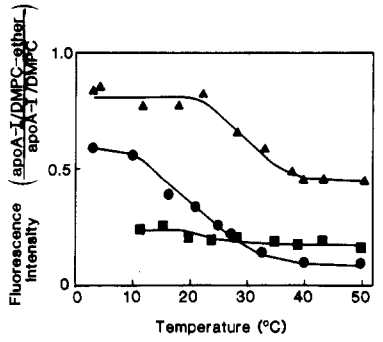

FIGURE 5: Temperature dependence of the relative quantum yields of Prodan (■), pyrene (●), and DPH (▲) in apoA-I/DMPC ether compared to that in apoA-I/DMPC recombinants as a function of temperature. The relative quantum yield is obtained by dividing the intensity value in the DMPC ether complex by the intensity value in the DMPC complex.

a change in the microenvironment surrounding the probe as the sample was heated above the phase transition temperature was indicated by a decrease in the enhancement ratio (Figure 4). At each temperature, the ratios for the model HDL decreased in the order apoA-I/DMPC > apoA-I/DMPC ether > DMPC > DMPC ether.

The relative fluorescence quantum yields of pyrene, DPH, and Prodan were measured as a function of temperature in model HDL containing DMPC and DMPC ether (Figure 5). For all three probes, the relative quantum yields were lowered when the probes were transferred from a DMPC ester matrix to one composed of DMPC ether and when the matrix was heated from the gel to the liquid-crystalline phase (Table I).

DISCUSSION

The sequence of interactions necessary for the catalytic action of enzymes that utilize phospholipids for substrates is poorly understood because the properties of the lipid–water interface are radically changed by enzymic decomposition of the surface. The inertness of dialkylglycerophospholipids to enzymic hydrolysis makes them ideal surfaces for these studies, provided their properties are comparable to those of the corresponding diacylglycerophospholipids. By inspection of molecular models, it is evident that the absence of the carbonyl group could potentially decrease the molecular surface areas of glycerophospholipids and consequently the hydration of the lipid–water interface.

The carbonyl region ["hydrogen-belt region" (Brockerhoff, 1982)] of a phospholipid has properties which are distinct from those of the hydrophobic chain and polar head-group regions. Water penetration into the carbonyl region of the phospholipid bilayers has been demonstrated by several independent techniques. These include NMR (Schmidt et al., 1977), neutron scattering (Buldt et al., 1978; Zaccai et al., 1979), DSC (Blume, 1983), and capacitance (Ashcroft et al., 1981) measurements. In a liquid-crystalline state, the carbonyl region has a moderate polarity that resembles ethanol (ϵ = 20–25) (Bellemare & Fragata, 1980; Ashcroft et al., 1981; Zachariasse et al., 1981; Vaz et al., 1978). The hydration of the polar head group of PCs increases in the transition from a gel to a liquid-crystalline state (Lis et al., 1982; Guldbrand et al., 1982; Watts et al., 1978; Katz & Diamond, 1974). The increase in bound water is presumably a consequence of lateral expansion of the head-group region (Watts et al., 1978).

The fluorescence spectral properties of Prodan are highly dependent on solvent polarity. However, in a rigid media, the emission maxima can depend on both the polarity and the structural relaxation of polar groups surrounding the probe (Demchenko, 1982). The fluorescence properties of pyrene are determined by probe–polar group molecular interactions formed in the ground electronic state and are not affected by solvent relaxation (Georghiou & Mukhopadhyay, 1981). Thus, the spectral responses of the two probes monitor their microenvironments through two different mechanisms.

The fluorescence emission spectra of Prodan indicate different environments for the probe in gel and liquid-crystalline lipid (Figure 3). Above and below the phase transition, $\Delta\nu_{1/2}$ is close to its minimal value observed in pure solvents. This spectral homogeneity suggests that a single microenvironment is observed in each phase. In the temperature range of the phase transition, both microenvironments seem to be present as evidenced by maxima in the $\Delta\nu_{1/2}$ values. A variety of chemical and macromolecular lipid structures, including changes in the fatty acid or polar head-group composition, produced no significant change in Prodan fluorescence. The major changes that are observed are produced by differences in the physical state of the phospholipids (Table II). One major question is whether the spectral shifts are due to microenvironments which are produced by differences in solvent polarity or solvent relaxation. In systems where structural relaxation is important, the fluorescent probe exhibits a red shift in the emission maxima with increasing excitation wavelength (Demchenko, 1982; Lakowicz et al., 1983a,b). Red-edge excitation selectively excites those fluorophores which are surrounded by solvent molecules that are oriented in a configuration comparable to that found in a solvent-relaxed state. Thus, red-edge excitation can distinguish between a polarity shift and a "rigidity" shift. As shown in Figure 2, changing the excitation wavelength did not produce a significant red shift when measured in a model HDL at 15 or 45 °C. This behavior is in contrast to that of Patman in DOPC SBV, which exhibits a large red shift at 2 °C whereas none is observed at 22 or 50 °C (Lakowicz et al., 1983a); all temperatures are above the T_c for this phospholipid. In Figure 3, the spectra at 30 °C, which are broad ($\Delta\nu_{1/2}$ = 5500 cm^{-1}), indicate a shift in the wavelength maximum with increasing excitation wavelength, but this appears to be due to preferential excitation of the probes in a liquid-crystalline environment as compared to solvent relaxation. Moreover, the phase-sensitive fluorescence spectra of Patman in DMPC SBV suggest that the emission maxima from the measured relaxed state in gel-phase lipid are blue shifted (~20 nm) as compared to liquid-crystalline lipid (Lakowicz et al., 1983a). Thus, in gel and liquid-crystalline phospholipid, the probe does appear to reside in different microenvironments that have different polarizabilities.

Assuming Prodan emission spectral shifts are due predominantly to polarity differences, an environment similar to ethanol as a matching solvent is seen in the liquid-crystalline phase. This agrees with other reports based upon spectroscopic criteria (Ashcroft et al., 1981; Zachariasse et al., 1981; Vaz et al., 1978) and chemical reactivity (Bellemare & Fragata, 1980). The gel phase is less polar and has a matching solvent of ethyl acetate, a solvent which presumably would mimic the environment of a carbonyl group in a hydrophobic environment. Differences in a microenvironment of pyrene (Figure 4) are demonstrated by the emission enhancement ratio in going from gel to liquid-crystalline phospholipid. However, this spectral characteristic of pyrene does not directly correlate with solvent polarity because pyrene can form ground-state complexes with alcohols and esters that can alter its fluorescence spectra (Lianos & Georghiou, 1979; Nakajima, 1971).

The expected differences in hydration of gel and liquid-crystalline phase lipid suggest that the probes accurately reflect hydration differences in the microenvironments. Cholesterol modulates the depth of water penetration (Simon et al., 1981) and decreases the polarity of the bilayer (Kao et al., 1978). The observed effects of cholesterol on Prodan fluorescence are dose dependent and are consistent with a decrease in the hydration of the probe environment. In general, the properties of fluorescence probes in ether and ester PCs are similar, suggesting that it is the entry or exclusion of water from the interfacial region and not the influence of the carbonyl group that produces the altered microenvironment.

At 15 and 37 °C, Prodan partitions into single-bilayer vesicles and model HDL consisting of DMPC and DMPC ether with essentially identical free energies. This is surprising since the microenvironments of the probe as determined by fluorescence emission maxima and quantum yields are different in the two lipid matrices and are also different for the same matrix at 15 and 37 °C. The most sensitive measurements of differences in ether and ester PCs are the quantum yields of the probes (Figure 5). The quantum yield for Prodan in a model HDL consisting of DMPC ether is identical with that in buffer whereas for DMPC it is increased by a factor of 4–5 (Table I). With the absence of carbonyl dipoles, the interfacial region containing ether PCs should be less polar than their ester analogues. However, the relative polarity and the free energy of transfer indicate that the probes should have similar microenvironments. We suggest that the hydrophobic–hydrophilic interface is maintained in the ether lipids by more water penetration. The differences in quantum yields are due to the differences in the relative amounts of water present, with gel-phase lipid being less hydrated than that in the liquid-crystalline phase.

Conclusions. On the basis of a number of spectroscopic and thermodynamic criteria, the interfacial regions of PCs and their ether analogues are similar. The main distinction between the two lipids is that the interfacial region of ether lipids contains more water. Evidently, the competing effects of lateral interaction of acyl or alkyl chains and the spreading of the monolayer produced by the crowded head groups are the main determinants of the conformation of both lipids. We speculate that additional water molecules in ether PCs may replace the space occupied by the carbonyl group. The most important point, however, is the similarity in the affinity (K_p) of Prodan for the surfaces of PCs and PC ethers. This finding suggests that proteins and other amphiphiles that partition into the lipid surface via the hydrophobic effect will not distinguish between PCs and PC ethers.

ACKNOWLEDGMENTS

We thank Sarah Myers-Fossett and Marjorie Sampel for preparation of the manuscript and Susan Kelly for preparation of the line drawings.

Registry No. DMPC, 18194-24-6; DMPG, 28874-52-4; DMPC ether, 36314-48-4; DLPC, 18194-25-7; DPPC, 63-89-8; cholesterol, 57-88-5.

REFERENCES

Ashcroft, R. G., Coster, H. G. L., & Smith, J. R. (1981) *Biochim. Biophys. Acta 643*, 191.

Barenholz, Y., Gibbes, D., Litman, B. J., Gall, J., Thompson, T. E., & Carlson, F. D. (1977) *Biochemistry 16*, 2806.

Bartlett, D. R. (1959) *J. Biol. Chem. 234*, 466.

Bellemare, F., & Fragata, M. (1980) *J. Colloid Interface Sci. 77*, 243.

Blume, A. (1983) *Biochemistry 22*, 5436.

Brockerhoff, H. (1982) *Lipids 17*, 1001.

Buldt, G., Gally, H. U., Seelig, A., Seelig, J., & Zaccai, G. (1978) *Nature (London) 271*, 182.

Demchenko, A. P. (1982) *Biophys. Chem. 15*, 101.

Eibl, H. (1981) in *Liposomes: From Physical Structure to Therapeutic Application* (Knight, C. G., Ed.) p 19, Elsevier/North-Holland Publishing Co., Amsterdam.

Georghiou, S., & Mukhopadhyay, A. K. (1981) *Biochim. Biophys. Acta 645*, 365.

Griffith, O. H., Dehlinger, P. J., & Van, S. P. (1974) *J. Membr. Biol. 15*, 159.

Guldbrand, L., Johnson, B., & Wennerstrom, H. (1982) *J. Colloid Interface Sci. 89*, 532.

Jonas, A., & Mason, W. R. (1981) *Biochemistry 20*, 3801.

Kao, Y. J., Soutar, A. K., Hong, K.-Y., Pownall, H. J., & Smith, L. C. (1978) *Biochemistry 17*, 2689.

Katz, Y., & Diamond, J. M. (1974) *J. Membr. Biol. 17*, 87.

Lakowicz, J. R., Bevan, D. R., Maliwal, B. P., Cherek, H., & Balter, A. (1983a) *Biochemistry 22*, 5714.

Lakowicz, J. R., Thompson, B., & Cherek, H. K. (1983b) *Biochim. Biophys. Acta 734*, 299.

Lianos, P., & Georghion, S. (1979) *Photochem. Photobiol. 29*, 843.

Lis, L. J., McAlister, M., Fuller, N., Rand, R. P., & Parsegian, V. A. (1982) *Biophys. J. 37*, 657.

Mantulin, W. W., Massey, J. B., Gotto, A. M., Jr., & Pownall, H. J. (1981) *J. Biol. Chem. 286*, 1815.

Massey, J. B., Gotto, A. M., Jr., & Pownall, H. J. (1981) *Biochemistry 20*, 1979.

Matz, C. E., & Jonas, A. (1982) *J. Biol. Chem. 257*, 4535.

Misiorowski, R. L., & Wells, M. A. (1974) *Biochemistry 13*, 4921.

Nakajima, A. (1971) *Bull. Chem. Soc. Jpn. 44*, 3372.

Pownall, H. J., Pao, Q., Hickson, D., Sparrow, J. T., Kusserow, S. K., & Massey, J. B. (1981a) *Biochemistry 20*, 6630.

Pownall, H. J., Hickson, D., & Gotto, A. M., Jr. (1981b) *J. Biol. Chem. 256*, 9849.

Pownall, H. J., Van Winkle, W. B., Pao, Q., Rohde, M., & Gotto, A. M., Jr. (1982a) *Biochim. Biophys. Acta 713*, 496.

Pownall, H. J., Pao, Q., Hickson, D. L., Sparrow, J. T., & Gotto, A. M. (1982b) *Biophys. J. 37*, 175.

Reichardt, C. (1979) *Angew. Chem., Int. Ed. Engl. 18*, 98.

Schmidt, C. F., Barenholz, Y., Huang, C., & Thompson, T. E. (1977) *Biochemistry 16*, 3948.

Shen, B. W., Scanu, A. M., & Kezdy, F. J. (1977) *Proc. Natl. Acad. Sci. U.S.A. 74*, 837.

Simon, S. A., McIntosh, T. J., & Latorre, R. (1981) *Science (Washington, D.C.) 216*, 6567.

Sklar, L. A. (1980) *Mol. Cell. Biochem. 32*, 169.
Tall, A. R., Small, D. M., Shipley, G. G., & Lees, R. S. (1975) *Proc. Natl. Acad. Sci. U.S.A. 72*, 4940-4942.
Vaz, W. L. C., Nicksch, A., & Jahnig, F. (1978) *Eur. J. Biochem. 83*, 299.
Watts, A., Marsh, D., & Knowles, P. F. (1978) *Biochemistry 17*, 1792.
Weber, G., & Farris, F. J. (1979) *Biochemistry 18*, 3075.
Zaccai, G., Buldt, G., Seelig, A., & Seelig, J. (1979) *J. Mol. Biol. 134*, 693-706.
Zacchariasse, K. A., Phuc, N. V., & Kozankiewicz, B. (1981) *J. Phys. Chem. 85*, 2676.

Biosynthesis of Glycosphingolipids by Human Myeloid Leukemia Cells†

Joanne Buehler,‡ Eileen Qwan,‡ Michael W. DeGregorio,§ and Bruce A. Macher*,‖

Cancer Research Institute and Department of Pharmaceutical Chemistry, University of California, San Francisco, San Francisco, California 94143, and Children's Cancer Research Institute, Pacific Presbyterian Medical Center, San Francisco, California 94115

Received March 29, 1985

ABSTRACT: We have performed comparative studies of the neutral glycosphingolipids synthesized by three human myeloid leukemia cell lines, K562, KG1, and HL-60, which were metabolically labeled with [^{14}C]galactose, to evaluate changes in neutral glycosphingolipid synthesis with myeloid cell differentiation. Individual neutral glycosphingolipids containing one to four sugars were purified by a combination of the following methods: diethylaminoethyl-Sephadex column chromatography, acetylation–Florisil column chromatography, and high-performance liquid chromatography using an Iatrobead column. Compounds with one sugar were analyzed by thin-layer chromatography on borate plates. This analysis showed that HL-60 cells synthesize only glucosylceramide, whereas K562 and KG1 cells synthesize predominately glucosylceramide, but also a small amount of galactosylceramide. Compounds with two to four sugars were characterized by treatment with exo- and endoglycosidases. The results showed that K562 and KG1 cells are similar to cells from patients with acute leukemia in expressing two series (globo and neolacto) of natural glycosphingolipids, whereas the HL-60 cells are similar to mature human myeloid cells in expressing only one series (neolacto). Therefore, human myeloid leukemia cells blocked at different stages of differentiation vary in their ability to synthesize neutral glycosphingolipids.

A number of biochemical changes are known to occur in leukocytes undergoing differentiation including altered expression of cell surface components. Our own work has been directed toward gaining information on the changes which occur in one class of cell surface glycoconjugates (glycosphingolipids) of human leukocytes. In the past few years, we have purified and structurally characterized the glycosphingolipids of normal human peripheral blood leukocytes and leukemia cells (Table I). These studies have demonstrated a number of differences in the glycosphingolipid composition of different populations of normal and leukemic leukocytes. With respect to neutral glycosphingolipids, we found that well-differentiated forms of human lymphoid cells [normal peripheral blood lymphocytes and chronic lymphocytic leukemia (CLL)[1] cells] contain only globo-type compounds, whereas well-differentiated forms of human myeloid cells (normal peripheral blood granulocytes and CML cells) contain neolacto- and gala-type compounds. Therefore, these two classes of well-differentiated human leukocytes, which are derived from a common stem cell precursor, express completely different classes of neutral glycosphingolipids. Our characterization of neutral glycosphingolipids from poorly differentiated human leukocytes (acute leukemia cells) has shown that, regardless of cell lineage, these cells all contain both globo and neolacto compounds. From these results, we have concluded that poorly differentiated leukocytes contain both neolacto and

Table I: Glycosphingolipid Structures

abbreviation	structure	name
GalCer	Galβ1→1Cer	galactosylceramide
GlcCer	Glcβ1→1Cer	glucosylceramide
Gal_2Cer	Galα1→4Galβ1→1Cer	galabiosylceramide
LacCer	Galβ1→4Glcβ1→1Cer	lactosylceramide
Gb_3Cer	Galα1→4Galβ1→4Glcβ1→-1Cer	globotriaosylceramide
Lc_3Cer	GlcNAcβ1→3Galβ1→-4Glcβ1→1Cer	lactotriaosylceramide
Gg_3Cer	GalNAcβ1→4Galβ1→-4Glcβ1→1Cer	gangliotriaosylceramide
Gb_4Cer	GalNAcβ1→3Galα1→-4Ga1β1→4Glcβ1→1Cer	globotetraosylceramide
nLc_4Cer	Galβ1→4GlcNAcβ1→-3Galβ1→4Glcβ1→1Cer	neolactotetraosylceramide

† This work was supported by Grant 1462 from the Council for Tobacco Research–U.S.A., Inc. (to B.A.M.), by Louis R. Lurie Foundation funds (to M.W.D.), and by National Cancer Institute Grant CA 32826 (to B.A.M.).

* Address correspondence to this author at the Cancer Research Institute, University of California, San Francisco.
‡ Cancer Research Institute.
§ Children's Cancer Research Institute.
‖ Cancer Research Institute and Department of Pharmaceutical Chemistry.

[1] Abbreviations: Cer, ceramide; CLL, chronic lymphocytic leukemia; CML, chronic myelogenous leukemia; DCE, dichloroethane; DEAE-Sephadex, diethylaminoethyl-Sephadex; GL_1, monohexosylceramide; GL_2, dihexosylceramide; GL_3, trihexosylceramide; GL_4, tetrahexosylceramide; GM_3, NeuAcα2→3Galβ1→4Glcβ1→1Cer; GM_2, GalNAcβ1→4(NeuAcα2→3)Galβ1→4Glcβ1→1Cer; GD_3, NeuAcα2→-8NeuAcα2→3Galβ1→4Glcβ1→1Cer; PBS, phosphate-buffered saline; TLC, thin-layer chromatography; HPLC, high-performance liquid chromatography; PPO, 2,5-diphenyloxazole.

0006-2960/85/0424-6978$01.50/0